Graphical Abstract

Preliminary Clinical Validation of 60 kVp Double-low-dose Coronary CT Angiography with A Deep Learning Reconstruction Algorithm

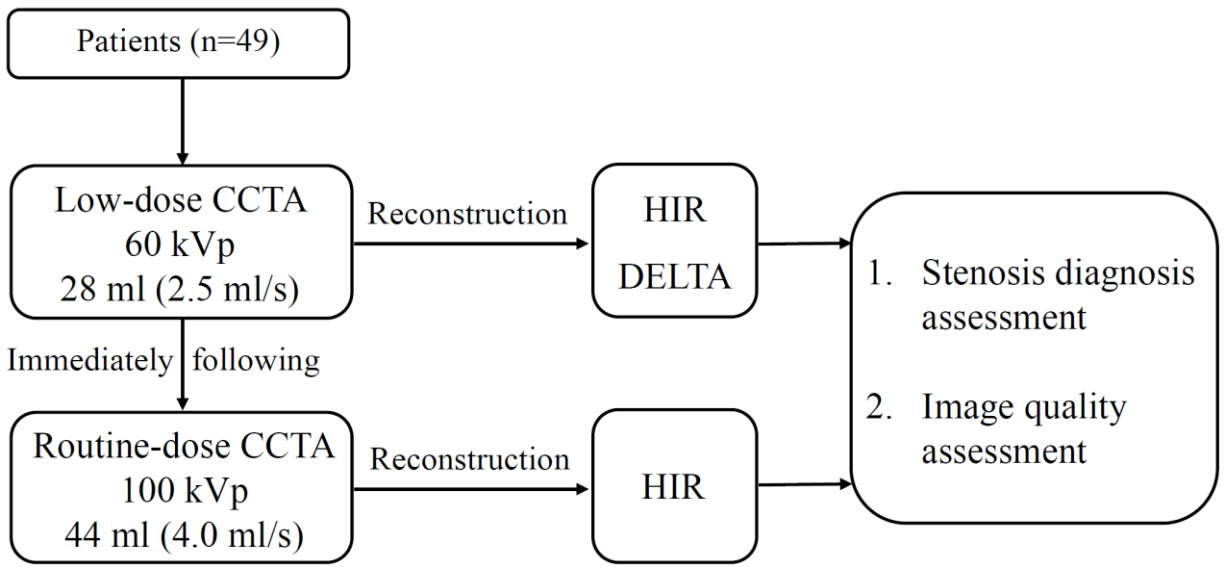

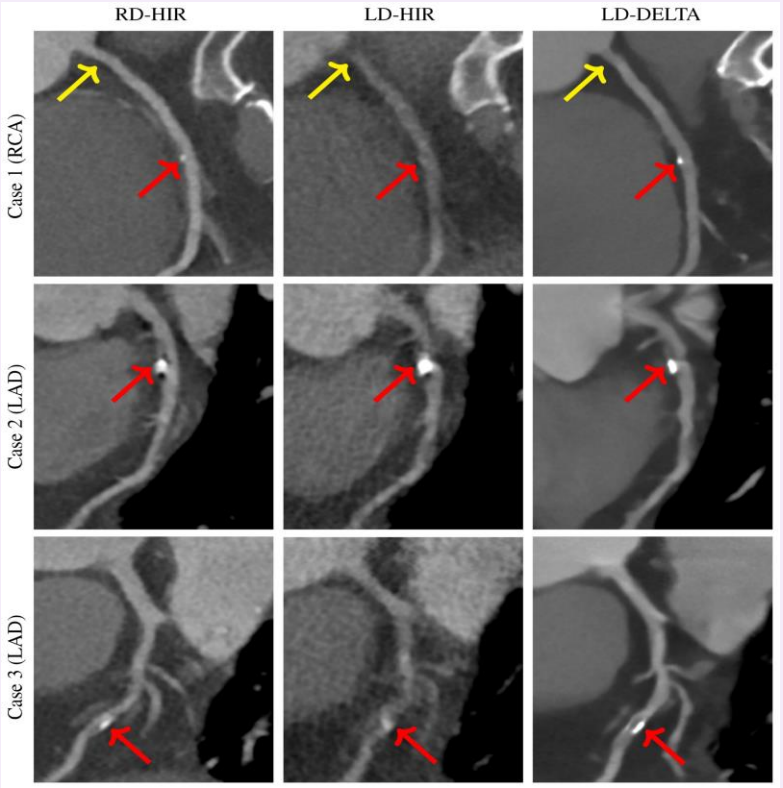

The radiation and contrast dose of 60 kVp CCTA protocol can be markedly reduced without compromising stenosis diagnostic performance.

Insights into Imaging

Insights Imaging (2025) Wu X et al. DOI: xxxx

Preliminary clinical validation of 60 kVp double-low-dose coronary CT angiography with a deep learning reconstruction algorithm

Abstract

Objectives To validate the clinical feasibility of 60 kVp double-low-dose coronary CT angiography (CCTA) with the DEep Learning Trained Algorithm (DELTA).

Methods Forty-nine patients (26 females, 58.6±14.9 years, 23.1±3.6 kg/m^2) with known or suspected coronary artery disease were prospectively enrolled. Each patient underwent the double-low-dose CCTA (60-kVp, 28ml contrast at 2.5ml/s) and immediately followed by routine-dose CCTA (100-kVp, 44ml contrast at 4.0ml/s). Routine-dose data was reconstructed using hybrid iterative reconstruction (RD-HIR), and low-dose data was reconstructed using both HIR (LD-HIR) and DELTA (LD-DELTA). The stenosis diagnostic performance of LD-HIR and LD-DELTA was analyzed at segment, vessel and patient levels using receiver operating characteristic analysis with the RD-HIR as reference. Segment-level image quality scores (IQS), signal-noise-ratio (SNR) and contrast-noise-ratio (CNR) were compared among three image sets.

Results Double-low-dose CCTA achieved significant reduction in both radiation dose (0.5±0.1 mSv vs. 4.0±1.2 mSv) and contrast volume compared to routine-dose CCTA. For per-segment level, LD-DELTA showed the significantly higher specificity (100.0% vs. 92.6%), positive predictive value (100.0% vs. 52.4%), accuracy (99.3% vs. 92.5%), accuracy-score (97.3% vs. 84.4%) and Kappa-score (0.94 vs. 0.65) compared to LD-HIR. The area under curve of LD-DELTA was significantly higher than LD-HIR at RCA-vessel (1.00 vs. 0.95), LCX-vessel (1.00 vs. 0.92), mid-segment (1.00 vs. 0.93) and distal-segment (1.00 vs. 0.97) levels. The IQS, SNR and CNR of LD-DELTA were not inferior to RD-HIR on all segments.

Conclusions The 60 kVp double-low-dose CCTA with the DELTA can significantly reduce radiation and contrast dose and simultaneously maintain diagnostic performance for stenosis assessment.

Critical Relevance Statement The 60 kVp double-low-dose coronary CT angiography protocol is feasible with a novel deep learning reconstruction algorithm without compromising diagnostic performance of coronary stenosis.

Key Points

- The 60 kVp double-low-dose coronary CT angiography (CCTA) protocol with a deep learning reconstruction (DLR) algorithm has been validated for routine clinical application.
- The radiation and contrast dose of 60 kVp CCTA protocol with the DLR algorithm can be markedly reduced by 86.7% and 36.4%, respectively.
- The 60 kVp double-low-dose CCTA protocol with the DLR algorithm obtained a high coronary stenosis diagnostic performance at segment-level, vessel-level and patient-level (all AUC ⩾ 0.94).

Keywords Coronary CT angiography; low-dose; deep learning reconstruction.

Abbreviations

CCTA	Coronary computed tomography angiography
CAD	Coronary artery disease
DLR	Deep learning reconstruction
ED	Effective dose
DELTA	DEep Learning Trained Algorithm
HIR	Hybrid iterative reconstruction
CTDIvol	Volume CT dose index
ROI	Region of interest
DLP	Dose-length product
RD-HIR	Routine-dose CCTA data reconstructed by the HIR algorithm
LD-HIR	Low-dose CCTA data reconstructed with the HIR algorithm
LD-DELTA	Low-dose CCTA data reconstructed with the DELTA

CAD-RADS	CAD-Reporting and Data System
ROC	Receiver operating characteristic
IQS	Image quality score
SNR	Signal-noise-ratio
CNR	Contrast-noise-ratio
SD	Standard deviation
PPV	Positive predictive value
NPV	Negative predictive value
BMI	Body mass index
AUC	Area under curve
HR	Heart rate
HRv	Heart rate variability
bpm	beats per minute
RCA	Right coronary artery
LAD	Left anterior descending
LCX	Left circumflex
CPR	Curved planar reconstruction
VR	Virtual-reality
CI	Confidence interval

Introduction

Coronary computed tomography angiography (CCTA) has become a widely adopted non-invasive imaging modality for rapid diagnosis of coronary artery disease (CAD), enabling detailed visualization of artery anatomy and assessment of stenosis [1, 2]. As reported by Kumar et al, CCTA obtained a high sensitivity and negative predictive value (both > 95%) with outstanding specificity for the detection of CAD [3]. And Machado et al found that CCTA can reduce need for the invasive coronary angiography (ICA) in 77% of patients with stable chest pain [4].

Due to the trend of younger onset of CAD, CCTA was widely employed a large

patient population [5], which raises concerns about its potential long-term risk of radiation-induced carcinogenesis [6]. This risk is particularly relevant in populations requiring CCTA follow-up, such as patients with previously diagnosed CAD and undergoing interventional treatment. In addition, the use of contrast agent poses a risk of inducing renal injury, especially for patients with renal insufficiency [7, 8]. As a result, reducing both radiation and contrast dose (termed as "double-low" strategy) while maintaining sufficient diagnosis image quality in CCTA has become a primary focus of current researches [9, 10, 11].

To address the common issue of heightened image noise in double-low strategy, the advanced deep learning reconstruction (DLR) algorithm was usually utilized to improve CCTA image quality. For example, Caruso et al studied the 80 kVp CCTA with the DLR algorithm protocol in non-obese patients, yield 42% mean effective dose (ED) reduction to 2.36 mSv [9]. Zhu et al explored 70 kVp CCTA with the DLR algorithm in normal-weight group and overweight group, achieving the reduced mean ED to 1.36 mSv and 1.59 mSv [10]. And Li et al researched the 70 kVp CCTA combined with a DLR algorithm reduced 50.6% contrast dose and 54.5% radiation dose to 0.75 mSv [11].

However, the lowest tube voltage setting currently available in clinical practice is 60 kVp, and 60 kVp CCTA combined with low-dose contrast agents has not been reported for its effectiveness in coronary imaging. Therefore, the aim of this study was to validate the feasibility of 60 kVp double-low-dose CCTA with a novel DEep Learning Trained Algorithm (DELTA) and explore the diagnostic performance of this protocol, compared to the conventional protocol of 100 kVp CCTA with the hybrid iterative reconstruction (HIR) algorithm.

Materials and methods

Participant enrollment

This study was approved by the local Institutional Review Board. From July 2024 to August 2024, 62 consecutive patients scheduled for CCTA due to known or suspected

CAD were prospectively enrolled, where the written informed consents were provided. Patients with nephropathy (n = 1), coronary stents (n = 5), history of bypass graft (n = 1), and incomplete raw data (n = 6) were excluded. All reconstructed CCTA images were reviewed to remove those with non-diagnostic quality due to high HR or arrhythmia. Consequently, 49 patients were included in this study for further assessment and analysis.

CCTA acquisition

All CCTA examinations were conducted with a 320-row detector scanner (uCT 960+, United Imaging Healthcare) with a prospective ECG-triggered axial scan mode. The phase range of data acquisition was between 30% and 80% in one R-R interval. Prior to the CCTA examination, all participants underwent breath-hold training and were administered 0.5 mg of sublingual nitroglycerin. Then, participants underwent the low-dose CCTA scanning immediately followed by the routine-dose CCTA scanning. The low-dose CCTA used a tube voltage of 60 kVp with a reduced contrast injection rate of 2.5 ml/s and a reduced total contrast volume of 28 ml. The routine-dose CCTA was performed with the tube voltage of 100 kVp with the contrast agent injection rate of 4.0 ml/s and the total contrast volume of 44 ml. The concentration of contrast agent (Iopromide) is 400 mg I/ml.

The other acquisition parameters were kept constant between both protocols: a collimation width of 280 × 0.5 mm, a rotation time of 0.25 s, and a reference exposure of 230 mAs. The prospective ECG-gating was applied with a threshold-triggering technique, placing the region of interest (ROI) in the descending aorta and setting the trigger threshold at 180 HU with a delay time of 2 seconds. The volume CT dose index (CTDIvol), dose-length product (DLP), and ED were recorded for both CCTA protocols. The ED was calculated as the DLP times a conversion factor for the chest $k = 0.014$ $mSv \times mGy^{-1} \times cm^{-1}$.

Image reconstruction and post-processing

After the data acquisition, the automatic phase selection algorithm (ePhase, United

Imaging Healthcare) was used to find the optimal phase in the full cycle for improving reconstruction image quality. The routine-dose CCTA data is reconstructed by the hybrid iterative reconstruction algorithm (RD-HIR) with level 7, while the low-dose CCTA data are reconstructed with both the HIR algorithm (LD-HIR) with level 9 and the DELTA (LD-DELTA) with denoising level 3. The HIR reconstruction adopted a standard soft kernel, and DELTA reconstruction adopted a standard sharp kernel. To further reduce motion artifacts, the artificial intelligence-assisted motion correction technique (CardioCapture, United Imaging Healthcare) with level 7 was utilized in three groups. All image reconstructions adopted a 512 × 512 matrix size, 0.5 mm slice thickness, and 0.5 mm slice interval. All reconstructed image volumes were qualitatively and quantitatively assessed on the routine clinical workstation (uWS-CT, United Imaging Healthcare).

Stenosis diagnosis assessment

The focus of this study is to distinguish between mild and moderate to severe stenosis on each segment of three main coronary arteries, including the right coronary artery (RCA), the left anterior descending (LAD), and the left circumflex (LCX). The RCA and LAD were divided into proximal, mid, and distal segments, while the shorter LCX was divided into proximal and distal segments [12]. The moderate or severe stenosis with a reduction of more than 50% in the lumen diameter was considered positive, while mild stenosis with narrowing less than 50% was considered negative. According to the CAD-Reporting and Data System (CAD-RADS) scores (0-5 points) [13], CAD-RADS $\geq$ 3 was considered positive, otherwise negative. After stenosis assessment of all segments, the vessel-level stenosis was defined as positive where any one segment in this coronary artery was positive. Similarly, the patient-level stenosis was defined as positive where any one coronary artery in this patient was positive. The stenosis diagnosis performance of LD-HIR and LD-DELTA were evaluated using the receiver operating characteristic (ROC) curve analysis, with RD-HIR as the reference.

To further provide a detailed stenosis diagnosis assessment, accuracy analysis based on CAD-RADS scores (accuracy-score) and Cohen's Kappa based on CAD-

RADS scores (Kappa-score) of LD-HIR and LD-DELTA was also calculated and compared, with RD-HIR as the reference. Similarly, the CAD-RADS score at one vessel determined with the maximum of all CAD-RADS scores at its segments, and the CAD-RADS score at one patient determined with the maximum of all CAD-RADS scores at three vessels.

Two radiologists, each with 7 years of experience, independently and blindly evaluated the stenosis condition of each segment in three groups. Multi-planar reconstruction was employed to analyze each segment in at least two orthogonal planes, supplemented by additional planes as necessary. And two radiologists were allowed to freely adjusts the setting of display window and zoomed the images to optimally review the stenosis. The final CAD-RADS scores were defined according to the unanimous agreement of two radiologists. Similarly, if there is a discrepancy of one point or more between the ratings of two radiologists, the third radiologist with a seniority of 12-year experience in cardiac radiology would review the controversial segments to provide a consensus decision.

Image quality assessment

The subjective image quality score (IQS) was further independently and blindly for each segment by two radiologists with 7-year experience using a 5-point Likert scale. Specifically, IQS = 5 represented excellent lumen enhancement with clear vessel boundary delineation, IQS = 4 represented good lumen enhancement with mostly clear boundary delineation, IQS = 3 represented acceptable lumen enhancement with suboptimal vessel boundary delineation, IQS = 2 represented inadequate lumen enhancement with obvious vessel blurring, and IQS = 1 represented poor lumen enhancement with severe vessel blurring. The final IQS for each segment was determined by unanimous agreement between the two radiologists. If the scores of two radiologists differ by one point or more, the third radiologist with 12 years of experience would review the controversial images to provide a consensus score.

The objective signal-noise-ratio (SNR) and contrast-noise-ratio (CNR) of each segment were independently measured by the third radiologist on manually selected

ROIs as follows: SNR=μ_{seg}/σ_{seg}, CNR=$(\mu_{seg}-\mu_{fat})/\sigma_{fat}$, where μ_{seg} and μ_{fat} are the mean CT value of each segment and fat tissue, and σ_{seg} and σ_{fat} represent the standard deviation (SD) of each segment and fat tissue. Specifically, ROIs for each vessel segment were selected as the largest cross-sectional areas (2-5 mm in diameter), avoiding calcified plaques. Fat ROIs (~5 mm in diameter) were chosen from chest fat regions at the level of the aortic root.

Statistical analysis

All statistical analyses were conducted using Python software (version 3.9) and R software (version 4.4.2). Before significance analysis, the Shapiro-Wilk test was used to check the normality of data, and all data didn't follow a normal distribution in this study. The CTDIvol, DLP and ED between the routine-dose and low-dose protocols were compared Wilcoxon signed rank test. The sensitivity, specificity and accuracy between LD-HIR and LD-DELTA were compared using McNemar's test. The positive predictive value (PPV), negative predictive value (NPV) and accuracy-score between LD-HIR and LD-DELTA were analyzed using the Chi-Square test (all expected frequencies > 5) or Fisher's Exact test (at least one expected frequency ≤ 5). The area under curve (AUC) was compared using Delong test. And the Kappa-score between LD-HIR and LD-DELTA were analyzed using the Z-statistic calculated from standard error. The Friedman test was used to analyze the difference of IQS, SNR and CNR among RD-HIR, LD-HIR and LD-DELTA, and post-hoc test adopted Dunn's test with Bonferroni correction for the comparison in any two groups. A p value < 0.05 was considered as statistical significance.

Results

Demographic characteristics and radiation dose

Forty-nine participants (26 females) were enrolled into the final analysis. As listed in Table 1, the average age was 58.6 ± 14.9 years and mean body mass index (BMI) was 23.1 ± 3.6 kg/m^2. There were some patients with chest pain (n = 21), hypertension

(n = 16), diabetes (n = 4), hyperlipidemia (n = 13), Smoking (n = 11), drink (n = 9), family history of CAD (n = 8), arrhythmia (n = 10), atrial fibrillation (n = 4), history of myocardial infarction (n = 3). The low-dose CCTA protocol demonstrated 86.7% reduction in radiation exposure compared to the routine-dose protocol, with significantly lower dose metrics: CTDIvol (2.9 ± 0.4 vs. 23.2 ± 9.2 mGy, $p < 0.001$), DLP (38.2 ± 8.1 vs. 286.5 ± 84.2 mGy·cm, $p < 0.001$), and effective dose (0.5 ± 0.1 vs. 4.0 ± 1.2 mSv, $p < 0.001$).

Diagnostic performance

Table 2 lists the overall stenosis diagnosis performance of LD-HIR and LD-DELTA at different level. For per-segment level, LD-DELTA showed the significantly higher specificity (100.0% vs. 91.6%, $p < 0.001$), PPV (100.0% vs. 51.6%, $p < 0.001$), accuracy (99.7% vs. 92.1%, $p < 0.01$), accuracy-score (96.4% vs. 83.7%, $p < 0.001$) and Kappa-score (0.90 vs. 0.60, $p < 0.001$) than LD-HIR. For per-vessel level, LD-DELTA achieved the significantly higher specificity (100.0% vs. 83.6%, $p < 0.001$), PPV (100.0% vs. 47.5%, $p < 0.001$), accuracy (99.3% vs. 85.7%, $p < 0.001$), accuracy-score (92.5% vs. 71.4%, $p < 0.001$) and Kappa-score (0.86 vs. 0.53, $p < 0.001$) compared to LD-HIR. For per-patient level, LD-DELTA obtained the significantly higher specificity (100.0% vs. 73.0%, $p < 0.01$), PPV (100.0% vs. 54.5%, $p < 0.05$), accuracy (98.0% vs. 79.6%, $p < 0.05$), accuracy-score (87.8% vs. 55.1%, $p < 0.001$) and Kappa-score (0.82 vs. 0.40, $p < 0.01$) than LD-HIR. There was no significant difference on sensitivity, NPV and AUC between LD-DELTA and LD-HIR at per-segment, per-vessel and per-patient levels (all $p > 0.05$).

Table 3 summarized the diagnosis performance of LD-HIR and LD-DELTA at different vessels. For RCA-vessel level, LD-DELTA achieved the significantly higher AUC (1.00 vs. 0.95, $p < 0.05$), accuracy-score (95.9% vs. 79.6%, $p < 0.05$) and Kappa-score (0.92 vs. 0.63, $p < 0.05$) than LD-HIR. For LAD-vessel level, LD-DELTA showed the significantly higher specificity (100.0% vs. 75.6%, $p < 0.01$), PPV (100% vs. 44.4%, $p < 0.05$), accuracy (98.0% vs. 79.6%, $p < 0.05$), accuracy-score (91.8% vs. 65.3%, $p < 0.01$) and Kappa-score (0.88 vs. 0.52, $p < 0.05$) compared to LD-HIR. For LCX-

vessel level, LD-DELTA obtained the significantly higher specificity (100% vs. 84.1%, $p < 0.05$), PPV (100% vs. 41.7%, $p < 0.05$), accuracy (100% vs 85.7%, $p < 0.05$), AUC (1.00 vs 0.92, $p < 0.01$), accuracy-score (95.9% vs. 87.1%, $p < 0.05$) and Kappa-score (0.84 vs. 0.57, $p < 0.001$) than LD-HIR. No significant difference existed on sensitivity, specificity, PPV, NPV and accuracy at RCA-vessel level, sensitivity, NPV and AUC at LAD-vessel level, and sensitivity and NPV at LCX-vessel level between LD-DELTA and LD-HIR (all $p > 0.05$).

Table 4 lists the stenosis diagnosis performance of LD-HIR and LD-DELTA at different segments. For proximal-segment level, LD-DELTA showed the significantly higher specificity (100% vs. 92.6%, $p < 0.01$), PPV (100% vs. 52.4%, $p < 0.01$), accuracy (99.3% vs. 92.5%, $p < 0.01$), accuracy-score (97.3% vs. 84.4%, $p < 0.001$) and Kappa-score (0.94 vs. 0.65, $p < 0.001$) than LD-HIR. For mid-segment level, LD-DELTA achieved the significantly higher specificity (100.0% vs. 86.4%, $p < 0.001$), PPV (100.0% vs. 45.5%, $p < 0.01$), accuracy (100.0% vs. 87.8%, $p < 0.001$), AUC (1.00 vs. 0.93, $p < 0.001$), accuracy-score (95.9% vs. 77.6%, $p < 0.001$) and Kappa-score (0.91 vs. 0.55, $p < 0.001$) compared to LD-HIR. For distal-segment level, LD-DELTA obtained the significantly higher specificity (100.0% vs. 94.1%, $p < 0.01$), PPV (100.0% vs 57.9%, $p < 0.05$), accuracy (100.0% vs 94.6%, $p < 0.01$), AUC (1.00 vs. 0.97, $p < 0.01$), accuracy-score (96.9% vs. 89.3%, $p < 0.05$) and Kappa-score (0.87 vs 0.64, $p < 0.01$) than LD-HIR. And there was no significant difference on sensitivity, NPV and AUC at proximal-segment level, and sensitivity and NPV at both mid-segment and distal-segment levels between LD-HIR and LD-DELTA (all $p > 0.05$).

Fig. 1 shows the curved planar reconstruction (CPR) images of RD-HIR, LD-HIR and LD-DELTA. For three groups, the CAD-RADS scores were 0 (negative), 1 (negative) and 0 (negative) at the proximal RCA marked by the yellow arrows and 1 (negative), 0 (negative) and 1 (negative) at mid RCA marked by the red arrows in case 1. And the scores were 2 (negative), 4 (positive) and 2 (negative) at proximal LAD marked by the red arrow in case 2, and were 2 (negative), 3 (positive) and 2 (negative) at mid LAD marked by the red arrow in case 3.

Image quality

Table 5 summarizes the objective IQS of RD-HIR, LD-HIR and LD-DELTA. The IQS in LD-HIR is significantly lower than both RD-HIR and LD-DELTA on all segments (all $p < 0.001$). And there is no significant difference on all segments between the IQS in LD-DELTA and RD-HIR (all $p > 0.05$).

Fig. 2 exhibits the whole coronary virtual-reality (VR) rendering and CPR images of RD-HIR, LD-HIR and LD-DELTA. The VR image of LD-DELTA shows a lot of recovered subtle vascular branches marked by red arrows, which are lost in that of LD-HIR. For CPR images in three groups, IQS were 5 vs. 4 vs. 5 at the proximal, mid and distal segments of RCA, 4 vs. 3 vs. 4 at the proximal LAD, proximal LCX and distal LCX, 5 vs. 3 vs. 5 at the mid LAD, and 4 vs. 3 vs. 5 at the distal LAD. LD-DELTA provides sharper vessel edges and clearer calcification plaque location than LD-HIR, which is close to or better than the visual image quality of RD-HIR.

Fig. 3 summarizes boxplot diagrams of SNR and CNR in RD-HIR, LD-HIR and LD-DELTA. LD-DELTA showed the significantly higher SNR and CNR than both RD-HIR and LD-HIR on all segments (all $p < 0.05$). There was no significant difference between RD-HIR and LD-HIR for SNR on distal segment of RCA ($p = 0.31$) and proximal segment of LAD ($p = 0.11$), while SNR on the others segments in LD-HIR was significantly lower than the RD-HIR (all $p < 0.05$). The CNR on distal LAD segment in LD-HIR was significantly lower than RD-HIR ($p < 0.05$), and had no significant difference on the others segments (all $p > 0.05$). Additionally, SNR were 22.4 ± 13.8 vs. 16.1 ± 12.6 vs. 36.8 ± 23.3 (all $p < 0.001$), and CNR were 25.1 ± 11.5 vs. 20.3 ± 10.6 vs. 62.1 ± 33.3 (all $p < 0.001$) in RD-HIR, LD-HIR and LD-DELTA at all segments (n = 392).

Discussion

This study investigated the feasibility of 60 kVp CCTA protocol combined with a novel DLR algorithm to reduce radiation and contrast agent dose and maintain the diagnosing performance of coronary stenosis, compared with the standard 100 kVp

CCTA with the HIR algorithm.

Compared to these previous low tube-voltage CCTA protocols, the studied 60 kVp CCTA protocol combined with the DLR algorithm obtained higher mean SNR of 36.8 and mean CNR of 62.1 with a lower mean ED of 0.53 mSv for patients with BMI < 31 kg/m^2. The mean SNR and mean CNR were 30.5 and 27.8 in the 80 kVp CCTA protocol for patients with BMI < 30 kg/m^2 [9], which were 35.3 and 47.6 in the 70 kVp CCTA protocol for patients with BMI < 26 kg/m^2 [11]. In addition, all assessments were conducted at segment-level, vessel-level and patient-level for the studied 60 kVp CCTA protocol to make a more detailed and comprehensive evaluation, while the previous 80 kVp or 70 kVp CCTA protocols only had qualitative and quantitative assessments at vessel-level.

There were still some limitations in this study. First, only coronary stenosis was evaluated in this work, others types of coronary diseases should be further assessed in 60 kVp CCTA protocol. Second, this study only analyzed the differentiation of mild and moderate to severe stenosis, and the accuracy of luminal stenosis assessment based on 60 kVp CCTA protocol may be decreased for patients with severe calcification, which need further research to validated. Third, although all patients in this research had no diagnostic gold standard of digital subtraction angiography, the accuracy of routine-dose CCTA had already been proven in tasks of coronary stenosis diagnosis [14, 15, 16]. Therefore, RD-HIR was taken as the reference for LD-HIR and LD-DELTA. Fourth, to ensure a high success rate of examination, the studied 60 kVp CCTA protocol only reduced 36.4% contrast dose to 28 ml. In the future, a personalized plan of low contrast agent dose should be attempted to further reduce the contrast dose.

In conclusion, this study demonstrated that the radiation and contrast dose of 60 kVp double-low-dose CCTA with the DELTA can be markedly reduced by 86.7% and 36.4% while maintaining the same or higher image quality and the high stenosis diagnostic performance with AUC ≥ 0.94 for patients with BMI < 31 kg/m^2, compared to the conventional 100 kVp CCTA with the HIR algorithm.

References

[1]. Abdelrahman K M, Chen M Y, Dey A K, et al (2020) Coronary computed tomography angiography from clinical uses to emerging technologies: JACC state-of-the-art review. Journal of the American College of Cardiology 76(10): 1226-1243

[2]. Bergamaschi L, Pavon A G, Angeli F, et al (2023) The role of non-invasive multimodality imaging in chronic coronary syndrome: anatomical and functional pathways. Diagnostics 13(12): 2083

[3]. Kumar V, Weerakoon S, Dey A K, et al (2021) The evolving role of coronary CT angiography in Acute Coronary Syndromes. Journal of Cardiovascular Computed Tomography 15(5): 384-393

[4]. Machado M F, Felix N, Melo P H C, et al (2023) Coronary computed tomography angiography versus invasive coronary angiography in stable chest pain: a meta-analysis of randomized controlled trials. Circulation: Cardiovascular Imaging 16(11): e015800

[5]. Wang S, Sun Z, Zeng Y et al (2024) Feasibility study of 'Triple-Low' technique for coronary artery computed tomography angiography (CCTA). Scientific Reports 14: 32110

[6]. LaBounty T M (2020) Reducing radiation dose in coronary computed tomography angiography: we are not there yet. JACC Cardiovascular Imaging 13: 435-436

[7]. Song P, Li K, Xu X, et al (2025) Impact of Cordyceps sinensis on coronary computed tomography angiography image quality and renal function in a beagle model of renal impairment. Frontiers in Pharmacology 16: 1538916. DOI: 10.3389/fphar.2025.1538916

[8]. Chua H R, Low S, Murali T M, et al. (2021) Cumulative iodinated contrast exposure for computed tomography during acute kidney injury and major adverse kidney events. European Radiology 31: 3258-3266

[9]. Caruso D, De Santis D, Tremamunno G, et al (2024) Deep learning reconstruction algorithm and high-concentration contrast medium: feasibility of a double-low protocol in coronary computed tomography angiography. European Radiology 35: 2213-2221

[10]. Zhu L, Ha R, Machida H, et al (2023) Image quality of coronary CT angiography at ultra low tube voltage reconstructed with a deep-learning image reconstruction algorithm in patients of different weight. Quantitative Imaging in Medicine and Surgery 13(6): 3891

[11]. Li W, Diao K, Wen Y, et al (2022) High-strength deep learning image reconstruction in coronary CT angiography at 70-kVp tube voltage significantly improves image quality and reduces both radiation and contrast doses. European Radiology 32(5): 2912-2920

[12]. Ansari U, Janssen S, Baumann S, et al (2023) Sparse 3D contrast-enhanced whole-heart imaging for coronary artery evaluation. Herz 48(1): 55-63

[13]. Cury R C, Leipsic J, Abbara S, et al (2022) CAD-RADS™ 2.0–2022 coronary artery disease-reporting and data system: an expert consensus document of the society of cardiovascular computed tomography (SCCT), the American college of cardiology (ACC), the American college of radiology (ACR), and the North America society of cardiovascular imaging (NASCI). Cardiovascular Imaging 15(11): 1974-2001

[14]. Serruys P W, Hara H, Garg S, et al (2021) Coronary computed tomographic angiography for complete assessment of coronary artery disease: JACC state-of-the-art review. Journal of the American College of Cardiology 78(7): 713-736

[15]. Han D, Liu J, Sun Z, Cui Y, He Y, Yang Z (2020) Deep learning analysis in coronary computed tomographic angiography imaging for the assessment of patients with coronary artery stenosis. Computer Methods and Programs in Biomedicine 196: 105651

[16]. Małota Z, Sadowski W, Pieszko K, et al (2023) The comparative method based on coronary computed tomography angiography for assessing the hemodynamic significance of coronary artery stenosis. Cardiovascular Engineering and Technology 14(3): 364-379

Table 1. Demographic data and clinical information of all participants
Data are mean ± SD (range) or % (n/N)
BMI body mass index, *HR* heart rate, *HRv* heart rate variability, *bpm* beats per minute, *CAD* coronary artery disease

Table 2. Table 2. The overall stenosis diagnosis performance of two low-dose coronary computed tomography angiography (CCTA) groups at segment-level, vessel-level and patient-level
PPV positive predictive value, *NPV* negative predictive value, *AUC* area under curve, *CI* confidence interval, *LD-HIR* low-dose CCTA data reconstructed by the hybrid iterative reconstruction algorithm, *LD-DELTA* low-dose CCTA data reconstructed by the DEep Learning Trained Algorithm

Table 3. The stenosis diagnosis performance of two low-dose CCTA groups on different vessels
RCA right coronary artery, *LAD* left anterior descending, *LCX* left circumflex

Table 4. The stenosis diagnosis performance of two low-dose CCTA groups on different segments

Table 5. The image quality scores of various segments in three groups
Data are mean ± SD
RD-HIR routine-dose CCTA data reconstructed by the hybrid iterative reconstruction algorithm

Figure 1. The curved planar reconstruction (CPR) images of three patients with different levels of coronary stenosis in three groups. Case 1-3 were the RCA vessel from one 59-year-old male, the LAD vessel from one 62-year-old male and the LAD vessel from another 62-year-old male

Figure 2. The whole virtual-reality (VR) rendering and the CPR images of various vessels on a 69-year-old female with diffuse calcification stenosis (positive on all segments) in three groups

Figure 3. The boxplot diagrams of signal-noise-ratio (SNR) and contrast-noise-ratio (CNR) on various segments from three different groups. The symbol “P”, “M” and “D” mean proximal, mid and distal segments. The “*”, “**” and “***” represent $0.01 \leq p < 0.05$, $0.001 \leq p < 0.01$ and $p < 0.001$, and “ns” means no significance

Table 1. Demographic data and clinical information of all participants

Characteristic	Overall (n = 49)
Female	53.1% (26/49)
Age (years)	58.6 ± 14.9 (17-93)
BMI (kg/m^2)	23.1 ± 3.6 (14.6-30.4)
HR (bpm)	74.1 ± 14.1 (50-106)
HRv (bpm)	7.6 ± 1.6 (5-12)
Chest tightness and pain	42.9% (21/49)
Hypertension	32.6% (16/49)
Diabetes	8.2% (4/49)
Hyperlipidemia	26.5% (13/49)
Smoking	22.4% (11/49)
Drink	18.4% (9/49)
Family history of CAD	16.3% (8/49)
Arrhythmia	20.4% (10/49)
Atrial fibrillation	8.2% (4/49)
History of myocardial infarction	6.1% (3/49)

Data are mean ± SD (range) or % (n/N)

BMI body mass index, *HR* heart rate, *HRv* heart rate variability, *bpm* beats per minute, *CAD* coronary artery disease

Table 2. The overall stenosis diagnosis performance of two low-dose coronary computed tomography angiography (CCTA) groups at segment-level, vessel-level and patient-level

Level	LD-HIR	LD-DELTA	*p* value
Per-segment (n = 392)			
Sensitivity % (n/N)	97.0% (32/33)	97.0% (32/33)	1.00
Specificity % (n/N)	91.6% (329/359)	100.0% (359/359)	< 0.001
PPV % (n/N)	51.6% (32/62)	100.0% (32/32)	< 0.001
NPV % (n/N)	99.7% (329/330)	99.7% (359/360)	1.00
Accuracy % (n/N)	92.1% (361/392)	99.7% (391/392)	< 0.001
AUC (95% CI)	0.94 ([0.91, 0.98])	0.98 ([0.96, 1.00])	0.07
Accuracy-score % (n/N)	83.7% (328/392)	96.4% (378/392)	< 0.001
Kappa-score	0.60	0.90	< 0.001
Per-vessel (n = 147)			
Sensitivity % (n/N)	100.0% (19/19)	94.7% (18/19)	1.00
Specificity % (n/N)	83.6% (107/128)	100.0% (128/128)	< 0.001
PPV % (n/N)	47.5% (19/40)	100.0% (18/18)	< 0.001
NPV % (n/N)	100.0% (107/107)	99.2% (128/129)	1.00
Accuracy % (n/N)	85.7% (126/147)	99.3% (146/147)	< 0.001
AUC (95% CI)	0.92 ([0.88, 0.95])	0.97 ([0.92, 1.00])	0.07
Accuracy-score % (n/N)	71.4% (105/147)	92.5% (136/147)	< 0.001
Kappa-score	0.53	0.86	< 0.001
Per-patient (n = 49)			
Sensitivity % (n/N)	100.0% (12/12)	91.7% (11/12)	1.00
Specificity % (n/N)	73.0% (27/37)	100.0% (37/37)	< 0.01
PPV % (n/N)	54.5% (12/22)	100.0% (11/11)	< 0.05
NPV % (n/N)	100.0% (27/27)	97.4% (37/38)	1.00
Accuracy % (n/N)	79.6% (39/49)	98.0% (48/49)	< 0.05
AUC (95% CI)	0.86 ([0.79, 0.94])	0.96 ([0.88, 1.00])	0.09
Accuracy-score % (n/N)	55.1% (27/49)	87.8% (43/49)	<0.001
Kappa-score	0.40	0.82	<0.01

PPV positive predictive value, *NPV* negative predictive value, *AUC* area under curve, *CI* confidence interval, *LD-HIR* low-dose CCTA data reconstructed by the hybrid iterative reconstruction algorithm, *LD-DELTA* low-dose CCTA data reconstructed by the DEep Learning Trained Algorithm

Table 3. The stenosis diagnosis performance of two low-dose CCTA groups on different vessels

Level	LD-HIR	LD-DELTA	*p* value
RCA (n = 49)			
Sensitivity % (n/N)	100.0% (6/6)	100.0% (6/6)	1.00
Specificity % (n/N)	90.7% (39/43)	100.0% (43/43)	0.13
PPV % (n/N)	60.0% (6/10)	100.0% (6/6)	0.23
NPV % (n/N)	100.0% (39/39)	100.0% (43/43)	1.00
Accuracy % (n/N)	91.8% (45/49)	100.0% (49/49)	0.13
AUC (95% CI)	0.95 ([0.91, 1.00])	1.00 ([1.00, 1.00])	< 0.05
Accuracy-score % (n/N)	79.6% (39/49)	95.9% (47/49)	< 0.05
Kappa-score	0.63	0.92	< 0.05
LAD (n = 49)			
Sensitivity % (n/N)	100.0% (8/8)	87.5% (7/8)	1.00
Specificity % (n/N)	75.6% (31/41)	100.0% (41/41)	< 0.01
PPV % (n/N)	44.4% (8/18)	100.0% (7/7)	< 0.05
NPV % (n/N)	100.0% (31/31)	97.6% (41/42)	1.00
Accuracy % (n/N)	79.6% (39/49)	98.0% (48/49)	< 0.05
AUC (95% CI)	0.88 ([0.81, 0.94])	0.94 ([0.82, 1.00])	0.40
Accuracy-score % (n/N)	65.3% (32/49)	91.8% (45/49)	< 0.01
Kappa-score	0.52	0.88	< 0.05
LCX (n = 49)			
Sensitivity % (n/N)	100.0% (5/5)	100.0% (5/5)	1.00
Specificity % (n/N)	84.1% (37/44)	100.0% (44/44)	< 0.05
PPV % (n/N)	41.7% (5/12)	100.0% (5/5)	< 0.05
NPV % (n/N)	100.0% (37/37)	100.0% (44/44)	1.00
Accuracy % (n/N)	85.7% (42/49)	100.0% (49/49)	< 0.05
AUC (95% CI)	0.92 ([0.87, 0.98])	1.00 ([1.00, 1.00])	< 0.01
Accuracy-score % (n/N)	87.1% (128/147)	95.9% (141/147)	< 0.05
Kappa-score	0.57	0.84	< 0.001

RCA right coronary artery, *LAD* left anterior descending, *LCX* left circumflex

Table 4. The stenosis diagnosis performance of two low-dose CCTA groups on different segments

Level	LD-HIR	LD-DELTA	*p* value
Proximal (n = 147)			
Sensitivity % (n/N)	91.7% (11/12)	91.7% (11/12)	1.00
Specificity % (n/N)	92.6% (125/135)	100.0% (135/135)	< 0.01
PPV % (n/N)	52.4% (11/21)	100.0% (11/11)	< 0.01
NPV % (n/N)	99.2% (125/126)	99.3% (135/136)	1.00
Accuracy % (n/N)	92.5% (136/147)	99.3% (146/147)	< 0.01
AUC (95% CI)	0.92 ([0.84, 1.00])	0.96 ([0.88, 1.00])	0.55
Accuracy-score % (n/N)	84.4% (124/147)	97.3% (143/147)	< 0.001
Kappa-score	0.65	0.94	< 0.001
Mid (n = 98)			
Sensitivity % (n/N)	100.0% (10/10)	100.0% (10/10)	1.00
Specificity % (n/N)	86.4% (76/88)	100.0% (88/88)	< 0.001
PPV % (n/N)	45.5% (10/22)	100.0% (10/10)	< 0.01
NPV % (n/N)	100.0% (76/76)	100.0% (88/88)	1.00
Accuracy % (n/N)	87.8% (86/98)	100.0% (98/98)	< 0.001
AUC (95% CI)	0.93 ([0.90, 0.97])	1.00 ([1.00, 1.00])	< 0.001
Accuracy-score % (n/N)	77.6% (76/98)	95.9% (94/98)	< 0.001
Kappa-score	0.55	0.91	< 0.001
Distal (n = 147)			
Sensitivity % (n/N)	100.0% (11/11)	100.0% (11/11)	1.00
Specificity % (n/N)	94.1% (128/136)	100.0% (136/136)	< 0.01
PPV % (n/N)	57.9% (11/19)	100.0% (11/11)	< 0.05
NPV % (n/N)	100.0% (128/128)	100.0% (136/136)	1.00
Accuracy % (n/N)	94.6% (139/147)	100.0% (147/147)	< 0.01
AUC (95% CI)	0.97 ([0.95, 0.99])	1.00 ([1.00, 1.00])	< 0.01
Accuracy-score % (n/N)	89.3% (142/159)	96.9% (154/159)	< 0.05
Kappa-score	0.64	0.87	< 0.01

Table 5. The image quality scores of various segments in three groups

Segments	RD-HIR	LD-HIR	LD-DELTA	*p* value
RCA (n = 49)				
Proximal	4.5 ± 0.5	3.4 ± 0.5	4.7 ± 0.5	< 0.001
Mid	4.4 ± 0.5	3.5 ± 0.6	4.7 ± 0.6	< 0.001
Distal	4.4 ± 0.6	3.5 ± 0.6	4.7 ± 0.5	< 0.001
LAD (n = 49)				
Proximal	4.4 ± 0.5	3.5 ± 0.6	4.7 ± 0.5	< 0.001
Mid	4.2 ± 0.5	3.2 ± 0.6	4.4 ± 0.6	< 0.001
Distal	4.0 ± 0.5	3.1 ± 0.7	4.3 ± 0.7	< 0.001
LCX (n = 49)				
Proximal	4.3 ± 0.6	3.3 ± 0.5	4.6 ± 0.5	< 0.001
Distal	3.9 ± 0.6	3.1 ± 0.5	4.3 ± 0.6	< 0.001

Data are mean ± SD

RD-HIR routine-dose CCTA data reconstructed by the hybrid iterative reconstruction algorithm

Figure 1.

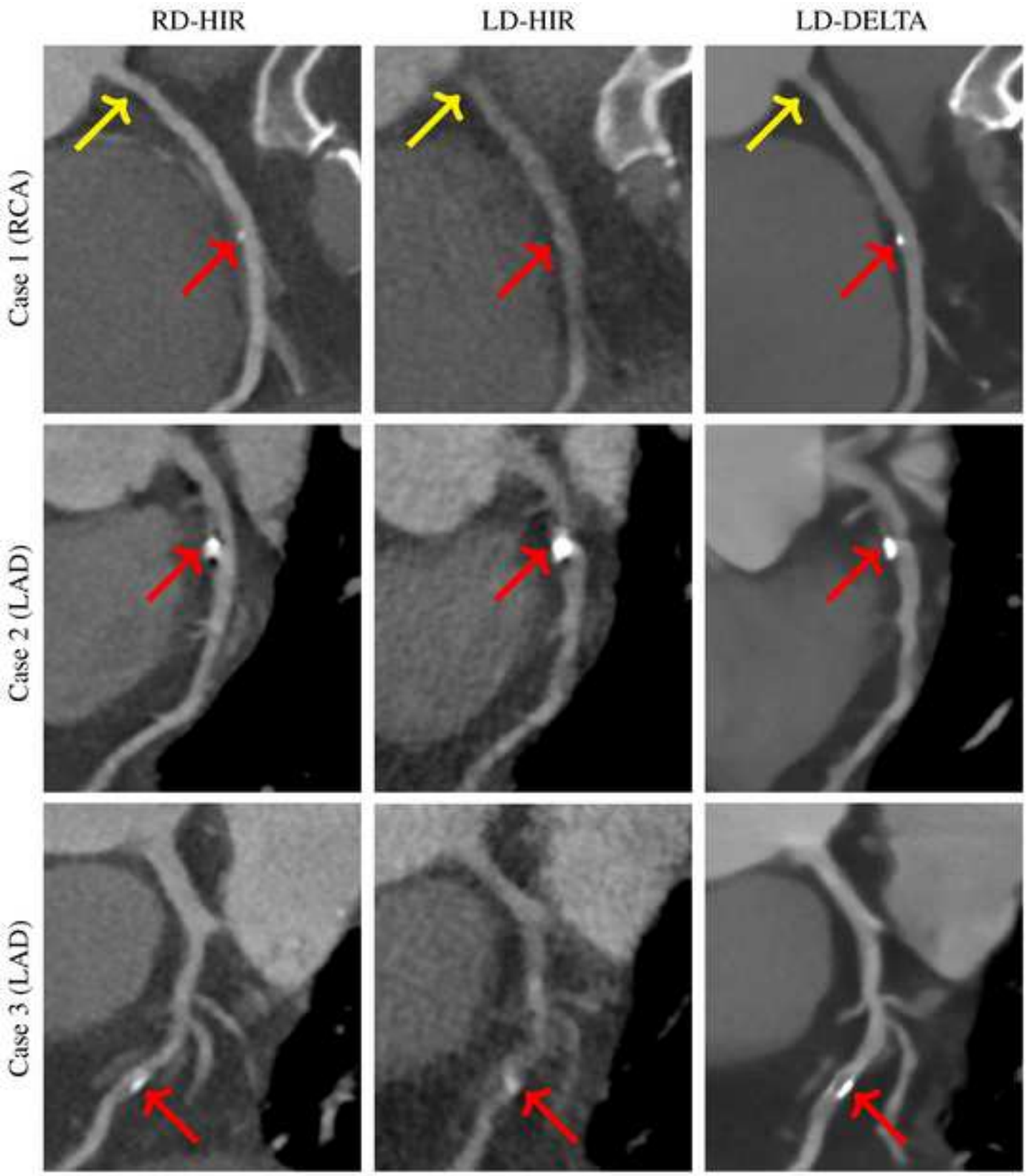

Figure 2.

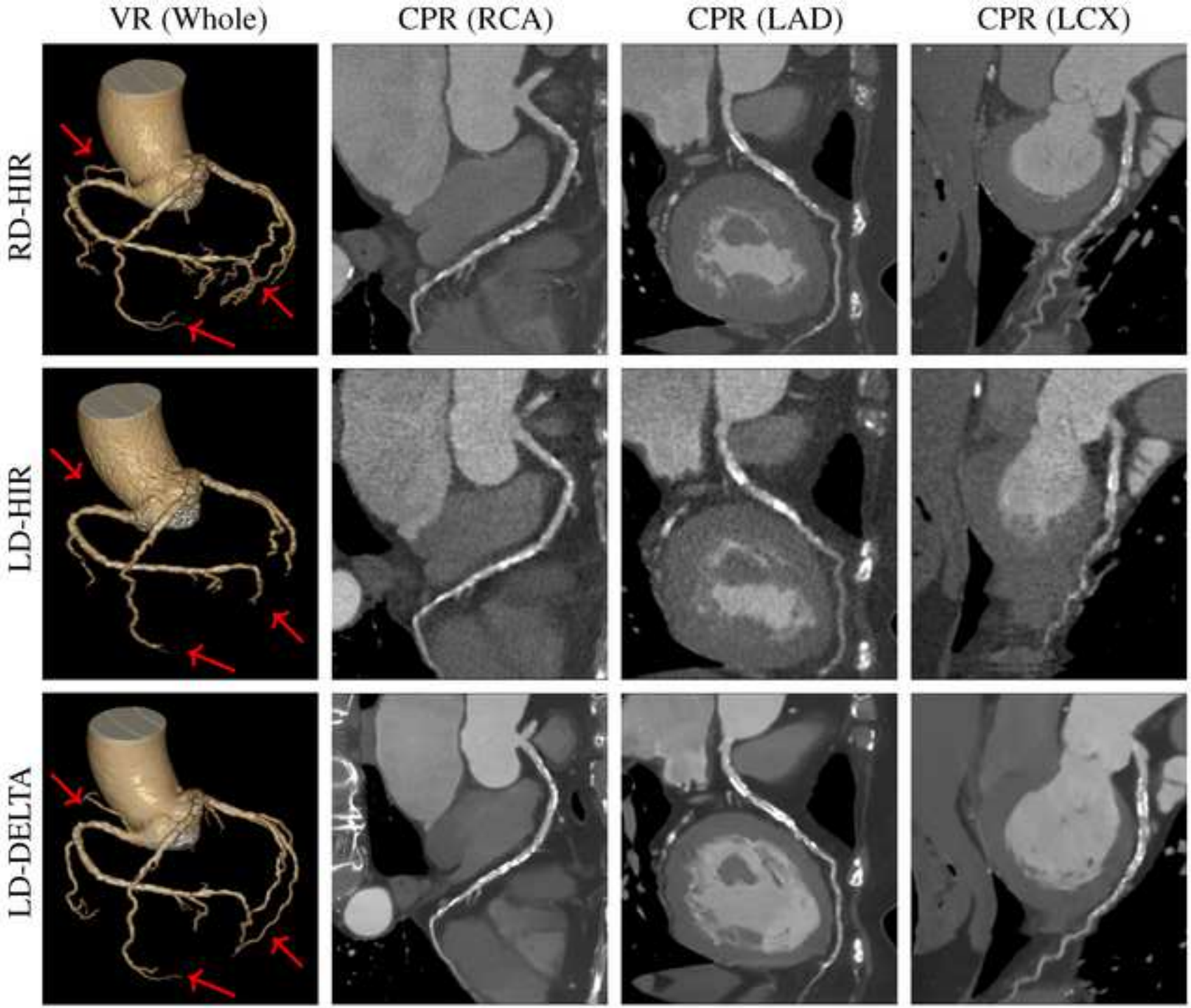

Figure 3.

Click here to access/download;Figure;Figure_3.tiff